MacHydro

# Upper Columbia Wetland Vulnerability Assessment –Final Report, Year 3 (2021-2022)

**A project of Kootenay Connect**

**Produced for:**
Dr. Suzanne Bayley
President of Columbia Wetlands Stewardship Partners

**March 29, 2022**

# Upper Columbia Wetland Vulnerability Assessment – Final Report, Year 3 (2021-2022)

**Suggested Citation:**

Goodbrand, A., MacDonald, R.J. (2022). Upper Columbia Wetland Vulnerability Assessment – Yr 3 Final Report. Prepared by MacDonald Hydrology Consultants Ltd for the Columbia Wetlands Stewardship Partners. 29 pp.

MacDonald Hydrology Consultants Ltd.
4262 Hilltop Cres.
Cranbrook, BC V1C 6W3
ryan.macdonald@machydro.ca
403-892-4510

# Executive Summary

MacDonald Hydrology Consultants (MacHydro) in collaboration with the Columbia Wetland Stewardship Partners (CWSP) conducted a project to evaluate wetland vulnerability and determine priority wetlands where management actions like conservation or mitigation should be implemented. The objectives of the hydrology subproject included: monitoring wetland water levels in 38 wetlands, characterizing the wetlands into types based on geomorphic and hydrometric data, constructing conceptual wetland water balances, evaluating how hydrometeorological conditions and wetland water levels may change under future simulated climate change projections, and describing the wetland vulnerability to climate change based on the conceptual understanding of predominant water sources and fluxes to inform future mitigation actions.

A framework of first-order controls and wetland variables were used to group the wetlands into three types based on the wetland's connectivity with the channel network: continuous connectivity, discontinuous connectivity and no connectivity. Wetlands with continuous connectivity (connected to the river via a gap in the levee) has a hydrograph response that fluctuates with the rise and fall of river stage . Wetlands with discontinuous connectivity (connected to the river, creek, adjacent wetland via a gap) respond after water rises above the elevation of a beaver dam (overdam flooding) or the bank in the gap (overbank flooding). Wetlands with no connectivity (no gap) respond after water rises above the elevation of the levee (overlevee flooding) and surface inflow/outflow is through unchannelized surface flow. These wetlands differ from the others because of a slow hydrograph recession, which is likely due to no apparent outlet.

Wetland water balances indicate that evaporation exceeds precipitation. Wetlands that have discontinuous connectivity (1:4.0) and no connectivity (1:4.1) had higher precipitation:evaporation ratios compared to those that are continuously connected (1:3.1).

Changes to wetland water balance components due to climate change was evaluated with two future scenarios generated from statistically downscaled climate scenarios under two representative concentration pathways (RCPs). RCP 4.5 corresponds to a scenario where carbon emissions stabilize by 2040, while RCP 8.5 represents a scenario with minimal greenhouse gas emission mitigation. The simulation was split into three 30-year periods (1990-2019, 2021-2050, 2051-2080) to understand shifting baselines and the range of variability.

Climate change scenarios project average annual air temperature increases for the study area (1.4 – 1.7°C by 2050, 2.4 – 3.6°C by 2080). Precipitation is projected to slightly increase (27 – 35 mm by 2050, 53 – 70 mm by 2080), but the change in the timing (and amount) and phase of precipitation will have the larger impact on wetland hydrology. There is an expected reduction in the fraction of annual precipitation as snow (4 – 6% by 2050, 9 – 14% by 2080). Reduction of snowfall at high-elevation would be critical for late-season streamflow. Already, Columbia River flows at Nicholson have declined 13% in recent decades (Brahney et al, 2017), with much of the decline in August (Moore et al., 2020).

Projected climate change would shift the watershed towards more rainfall-dominated runoff and result in earlier snowmelt and spring peak flows, which may change the timing and duration of overbank/overdam/overlevee flooding and the period of inundation. Wetlands that are more isolated from the main river channel (discontinuous connectivity or no connectivity) channel do not receive as much inflow during the maximum annual peak flows (flood <0.5 - 1 m) compared to those that are continuously connected (flood 2-3 m during maximum annual peak flow). Therefore, with projected climate change, the more isolated wetlands would flood less and there would be concerns that a wetland under an extended growing season with greater evapotranspiration rates would not retain as much standing water over the winter and be particularly vulnerable to climate change. Therefore, how well (e.g. duration, timing) a wetland is connected to the channel network and how connectivity varies with changes in streamflow will determine the vulnerability to climate change. Wetlands that have discontinuous connectivity or no connectivity would be the most vulnerable and most important to mitigate to maintain habitat quality and bioecological functioning of the wetland.

# Contents

## List of Figures



## List of Tables

# 1 Introduction

This project is being conducted by the Columbia Wetland Stewardship Partners (CWSP) to evaluate wetland vulnerability and determine priority wetlands where management actions like conservation or mitigation should be implemented. The objectives of the hydrology subproject include:

1. Monitoring of wetland water levels in 38 instrumented wetlands with HOBOs for Year 2 (2020/2021);
2. Further characterize wetland types developed and mapped in Year 1 using geomorphic and hydrologic data collected in collaboration with University of Waterloo students and statistical analyses;
3. Construct conceptual water balances by wetland type using aerial imagery and estimated bathymetric information to estimate volumetric water inputs and outputs and changes in wetland volume;
4. Evaluate how hydrometeorological conditions and wetland water levels may change under future simulated climate change ensemble projections for Representative Concentration Pathways 4.5 and 8.5; and,
5. Describe wetland vulnerability based on the conceptual understanding of predominant water sources and fluxes by wetland type to help inform future mitigation actions.

# 2 Methods

## 2.1 Study Area

The study area is the Upper Columbia Watershed between Columbia Lake and Golden, with field investigation focused on the north-central portion of this area (Figure 1). The study area encompasses high elevation mountain ranges including the Rocky Mountains to the east and the Columbia and Purcell Mountains in the west, separated by a deep post-glacial valley known as the Rocky Mountain Trench. The region extends from under 800 m above sea level (a.s.l.) in the Rocky Mountain Trench, to over 3,500 m a.s.l. at the highest mountain peaks in the Rocky Mountains. Total mean annual precipitation is around 450 mm. The region predominantly consists of coniferous forests below 2,200 m a.s.l. and alpine grasslands and talus above. Within the Rocky Mountain Trench, the Columbia River flows slowly, creating a braided system of wetlands within the wide valley.

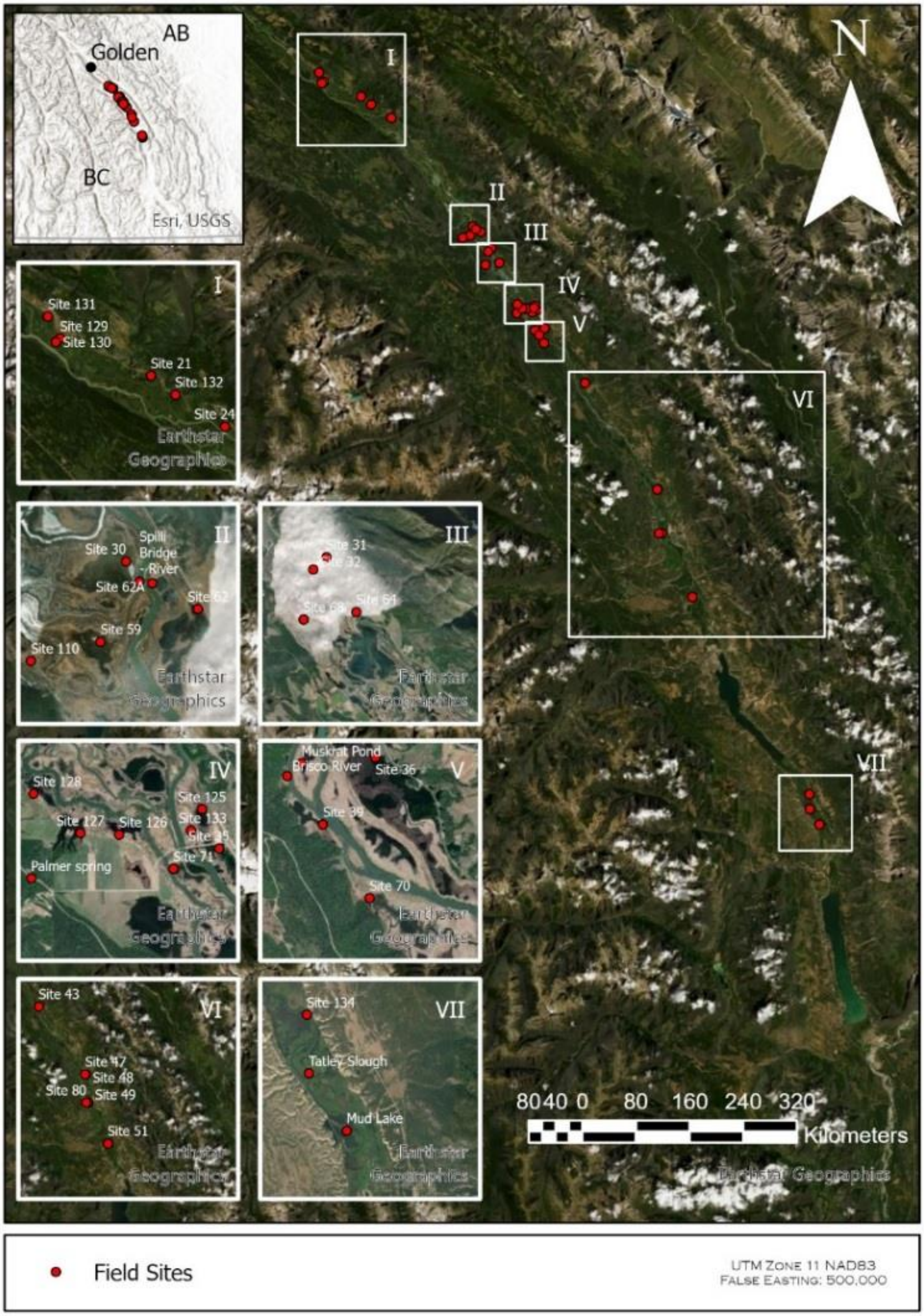


*Figure 1 Study area showing water level monitoring locations.*

## 2.2 Water Level Monitoring

Hobo U-20 level loggers were used to measure water level (m) at 38 individual wetlands, one site at Columbia River at Brisco, and one site along the Columbia River at the Spillamacheen Bridge (Figure 2). Water level loggers were installed from May 6 to May 11, 2021 and removed between October 16 and 21, 2021. Water levels were collected at 4-hour intervals and corrected with a barometric pressure sensor located at Brisco. The hobo logger at Wetland 63 malfunctioned and no data were collected. The hobo logger collecting water level in the Columbia River at Brisco was lost. Water levels collected in 2020 were previously reported (MacDonald Hydrology Consultants, 2021).

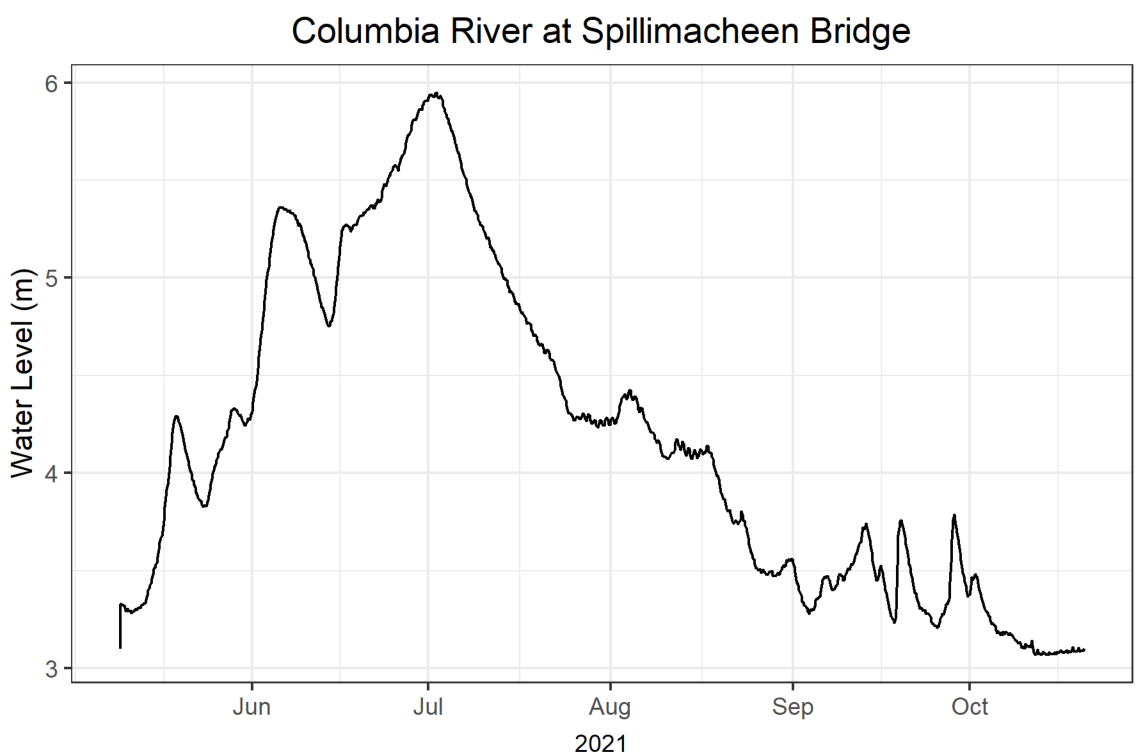


*Figure 2 Water levels in the Columbia River at the Spillimacheen Bridge in 2021.*

## 2.3 Principal Component Analysis

To explore and visualize differences in wetland groups, a Principal Component Analysis (PCA) was conducted using hydrograph variables, geomorphic characteristics, and wetland water conductivity (CondMay; collected in May, 2021).

The water level (WL) response of each wetland was analyzed using four hydrograph variables:

- Total change in storage from May 15 to October 15, 2021 (m):

$$Storage = \sum WL_{t-1} - WL_t \quad (1)$$

- Flashiness of hydrograph or how quickly the water level rises and falls (m):

$$Flashiness = \sum |WL_{t-1} - WL_t| \quad (2)$$

- Recession of first peak (cm $d^{-1}$):

$$Recession1 = (WL_{tpeak} - WL_{tqe})/(t_{peak} - t_{qe}) \quad (3)$$

where $qe$ is the end of the hydrograph response of the first peak

- Recession of maximum annual peak (cm $d^{-1}$):

$$Recession2 = (WL_{tpeak} - WL_{tqs})/(t_{qs} - t_{peak}) \quad (4)$$

where $qs$ is the end of the hydrograph response on October 15, 2021.

Geomorphic characteristics included: the count of beaver dams located within 10 m of the wetland (DamNo10), the total width of wetland gaps that allow river, creek, or between wetland water inflow or outflow (TFGapW), and the area of the wetland (Area). The stable water isotope data collected in 2019 and the subsequent evaporation:inflow ratios or estimates of the percentage of groundwater were not used in the analysis because only 20 of 38 wetlands were sampled (Remer et al., in prep). Rather water levels, geomorphic characteristics, and conductivity were used to develop a conceptual understanding of wetland water balances to infer the predominant water sources and fluxes to assist in identifying vulnerable wetlands. The range of continuous initial variables was standardized by subtracting the mean and dividing by the standard deviation for each value of each variable.

## 2.4 Wetland Grouping

The vulnerability of wetlands to changes in climate and land use is hypothesized to depend on their position within the hydrologic landscape; requiring an understanding of the relative role of the wetland's hydrologic connectivity to the stream network and their predominant hydrologic fluxes. A framework of first-order controls on wetland characteristics was used to develop a conceptual understanding of the water balance in each wetland type. The first-order controls include topography, topology, and typology (Buttle, 2006). Topography refers to the geomorphic setting of the wetland. Topology reflects the relative role of the wetlands in modulating water inputs from contributing slopes and a measure of the degree of hydrologic connectivity with the steam network. Topology also deals with whether a wetland shows continuous or discontinuous (both in time and space) hydrologic connectivity. Lastly, typology refers to the predominant hydrologic fluxes (vertical versus lateral) and characterizes the relative residence time of water held within wetlands before making its way to the stream channel.

## 2.5 Wetland Water Balances

A daily volumetric water balance was calculated from May 15 - September 30, 2020 and 2021 for all monitored wetlands via:

$$\Delta S = P - E + Qi - Qo + Gi - Go \quad (4)$$

where, ΔS was the change in wetland storage volume (m$^3$), *P* was precipitation as rainfall, *E* was actual evaporation (m$^3$), $Q_i$ was the inflow and $Q_o$ was the outflow of surface water (includes both channelized and unchannelized flow), and $G_i$ was the inflow and $G_o$ was the outflow of groundwater. The difference between water balance inputs and outputs was used to estimate the net volume of surface and groundwater flow (*Net*) for the wetland as these water balance terms were difficult to measure or estimate in the field. Therefore, the water balance was estimated via:

$$Net = \Delta S - P + ET \quad (5)$$

The *Net* term would also include any cumulative error in the measurement and calculation of the water balance components.

The total monthly (June, July, and August) and growing season (May 15 – September 30) volumetric water balances were calculated for each wetland. An area-weighted total monthly and growing season volumetric water balance were calculated for each wetland type (A, B, C, D, E). Water balances for 2020 data were only calculated for wetlands that were consistently monitored in 2021 and used to corroborate trends in 2021 water balances by wetland type (Appendix Table A2, Table A3, Figure A4). The water balance values were converted to mm by dividing by the total wetland area in the study area.

### 2.5.1 Wetland Storage

Daily water level records were used to calculate the change in wetland storage volume using volume – elevation curves. Hayashi and van der Kamp (2010) presented equations for estimating wetland volume for prairie potholes:

$$V = \frac{s}{(1 + 2/p)} \, x \, \frac{h^{(1+2/p)}}{h_o^{2/p}} \quad (6)$$

where *s* represents the size of the wetland (m$^2$), *p* is the depression profile, *h* is the depth of water (m) above the lowest point of the wetland ($h_{min}$), and $h_o$ is the unit depth (= 1 m). The *s* coefficient is the actual area of the wetland when the water depth is equal to the unit depth (h = 1 m). The *p* value is a power coefficient that represents the average slope profile of a wetland, where a large value corresponds to a basin with a flatter bottom. The p value was set to 50 to closely match the maximum surface area at the maximum wetland water level ($h_{max}$).

The maximum surface area of the wetland was delineated in ArcGIS using LiDAR imagery and orthophotos flown from September 11 to October 2, 2015 (work by Ryan Durand and Annie Pankovitch). We assumed the 2021 $h_{max}$ would equal the wetland's maximum surface area. To estimate $h_{max}$, a wetland survey conducted by University of Waterloo students in summer 2021 was used to estimate the lowest point in the wetland ($h_{min}$). The total water depth during the survey date was matched to the water level record at the staff gauge. The continuous water level record logged at the staff gauge was corrected if the staff gauge was not located at the $h_{min}$. The water level on September 21, 2021 was used to estimate the $h_{max}$ during a similar time period when the aerial imagery was collected (midpoint of aerial survey dates). We assume that the fall 2021 water level was like fall 2015. Stream discharge measured in the Columbia River at Nicholson (Climate ID 08NA002; 51° 14' 36" N 116° 54' 46" W) shows an average daily discharge for September 2015 at 117 $m^3 s^{-1}$, which falls close to the 103-year average daily discharge for September (103 $m^3 s^{-1}$, range 68 to 193) meaning the year of aerial imagery was not an extreme hydrologic year. Streamflow data for the hydrometric station was not yet available for 2021, but observations indicate 2021 was also not an extreme hydrologic year.

Wetland level changes also resulted in changes to their surface area ($m^2$), which influenced the amount of water evaporated from the pond. The daily change in wetland surface area was also calculated using the equation (Hayashi and van der Kamp, 2010):

$$A = s\left(\frac{h}{h_o}\right)^{2/p} \quad (7)$$

### 2.5.2 Precipitation

Rainfall data were obtained from the precipitation record at Brisco (FLNRO-WMB Brisco; Climate ID 865, 50.8193 N, -116.2449 W, elevation 930 m.a.s.l.). Data were missing or inconsistent from June 3 – 23, 2021. Daily precipitation was gap-filled using the relative (percentage) difference in monthly precipitation between Brisco and a nearby precipitation gauge at Panorama Ski Resort (MoTIe Panorama; Climate ID 37291, 50.46343 N -116.23348 W, elevation 1150 m.a.s.l.). The FLNRO-WMB Toby station near Invermere was also missing precipitation data during this time period. Rainfall volume was calculated by multiplying daily rainfall depth (m) by the maximum wetland surface area ($m^2$).

### 2.5.3 Open-Water Evaporation

Daily evaporation (m) from each wetland surface was calculated via the Penman (1948) method for open water (McMahon et al., 2013). Transpiration by wetland vegetation was not accounted for in this water balance. Longwave and shortwave radiation were estimated as outlined in Dingman (2002). Daily average minimum and maximum air temperature (°C), relative humidity (%), and wind speed ($m\ s^{-1}$) collected at the Brisco weather station were also used to estimate evaporation. Data were missing or inconsistent from June 3 – 23, 2021. These data were gap-filled using the climate station near Invermere (FLNRO-WMB Toby; Climate ID 417, 50.5128 N, -116.0553W, elevation 894 m.a.s.l.). Evaporation volume was calculated by multiplying daily evaporation by the pond surface area ($m^2$).

## 2.6 Wetland Vulnerability to Climate Change

Previous work from a semi-distributed hydrological model that was developed for the upper Columbia River Basin was used to evaluate how hydrometeorological conditions and wetland water balances may change under future climate change projections. The basin-scale model is an adapted version of the HBV-EC model, emulated within the Raven Hydrological Modelling Framework version 3.0 (Craig et al., 2020). The model simulates streamflow and other hydro-climatic variables (i.e., snowmelt, evaporation, etc.) at a daily timestep from 1980-2019. The model spatially distributes daily minimum and maximum air temperature and precipitation from all weather stations across the study region. The model simulates major hydrological processes including canopy interception, snow accumulation and melt, glacier melt, evaporation, soil infiltration, percolation, and baseflow, as well as surface runoff.

Model parameters were calibrated to the 2010-2018 period at Kicking Horse River at Golden and Columbia River at Nicholson. Model performance was verified over the remaining record (1987-2009) for sub-basins used in model calibration, and for the complete record for sites not used in calibration. Model performance statistics for daily streamflow simulated at Columbia River at Nicholson (downstream of the Columbia Wetlands) from the calibration period (Nash-Sutcliffe Efficiency = 0.88; Kling-Gupta Efficiency =0.76; Pearson Correlation Coefficient = 0.94; Percent Bias = 23.3) were similar to the verification period (Nash-Sutcliffe Efficiency = 0.89; Kling-Gupta Efficiency =0.88; Pearson Correlation Coefficient = 0.89; Percent Bias = 8.8).

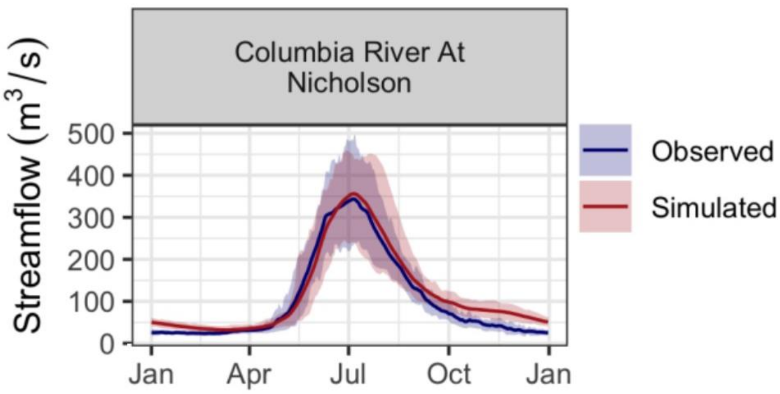


*Figure 3 Average daily hydrographs for the entire simulation period (1987 – 2019). Shaded areas correspond to the 10 – 90% quantiles, while the solid lines are the average.*

Changes to wetland water balance components due to climate change was evaluated with two future scenarios generated from statistically downscaled climate scenarios obtained from Environment and Climate Change Canada (ECCC, 2021) under two representative concentration pathways (RCPs). RCP 4.5 corresponds to a scenario where carbon emissions stabilize by 2040, while RCP 8.5 represents a scenario with minimal greenhouse gas emission mitigation. These scenarios applied the median projection from an equal-weighting ensemble forecast of 24 General Circulation Models (GCM) from the Coupled Model Inter-comparison Project Phase 5 (CMIP5) from 2021-2100. Projections among climate models can vary because of differences in their underlying representation of earth system processes. Thus, the use of a multi-model ensemble approach has been demonstrated in recent scientific literature to likely provide better projected climate change information (Zhang et al., 2019, ECCC, 2021). The simulation was split into three 30-year periods (1990-2019, 2021-2050, 2051-2080) to understand shifting baselines and the range of variability.

Daily future weather was generated by first bias-correcting projected climate values by calculating the change between simulated future air temperature and precipitation and historical (simulated). Each future month and year were then matched with a proxy month from the baseline (observed) period. These scaling factors for each month and year (i.e., fractional difference in precipitation and absolute difference in air temperature between the proxy and scenario) were then used these to correct the daily observed record for each climate scenario (Figure 4).

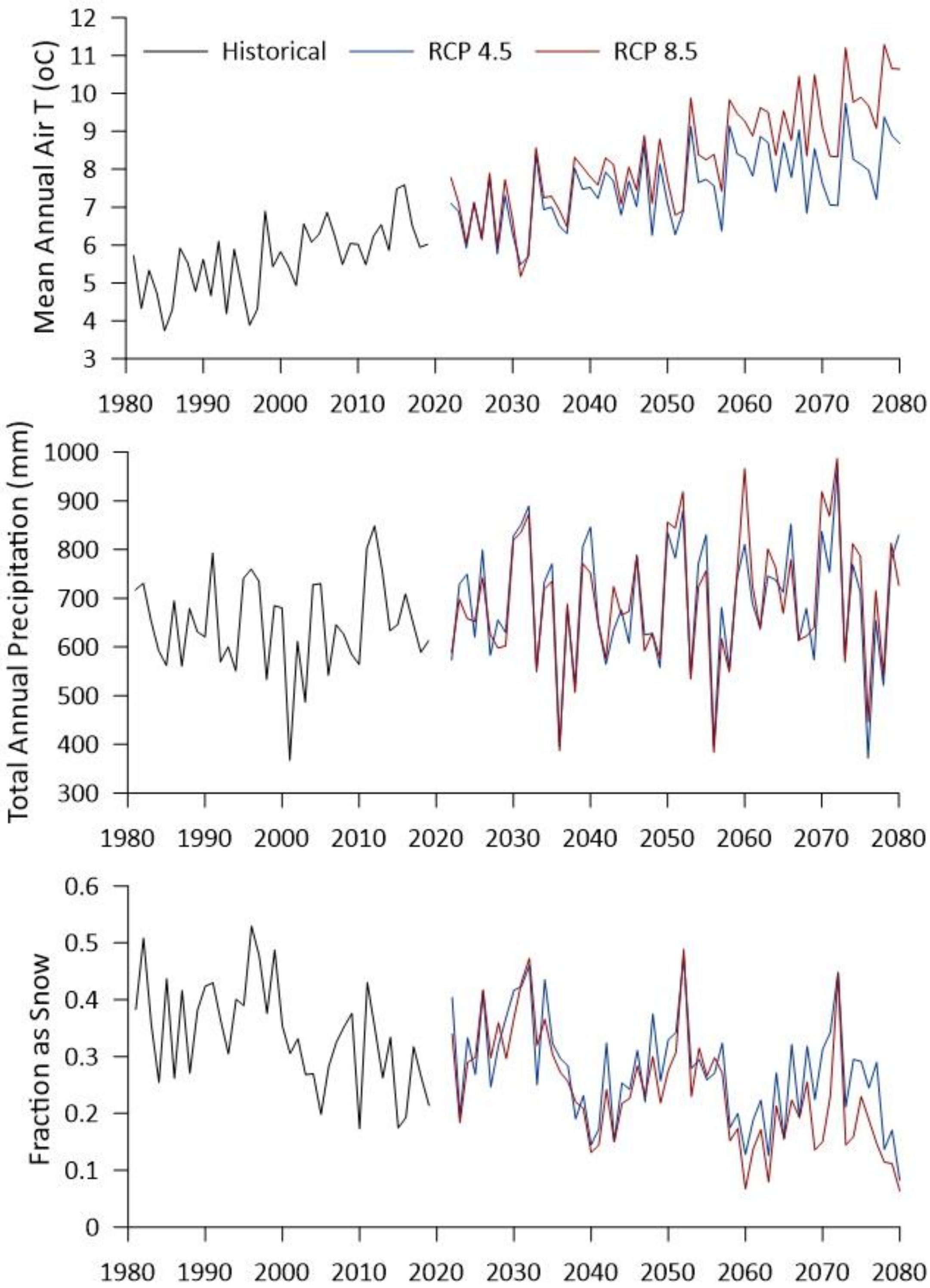


*Figure 4. Annual climate parameters under historical and future scenarios for the study area.*

# 3 Results

## 3.1 Water Levels

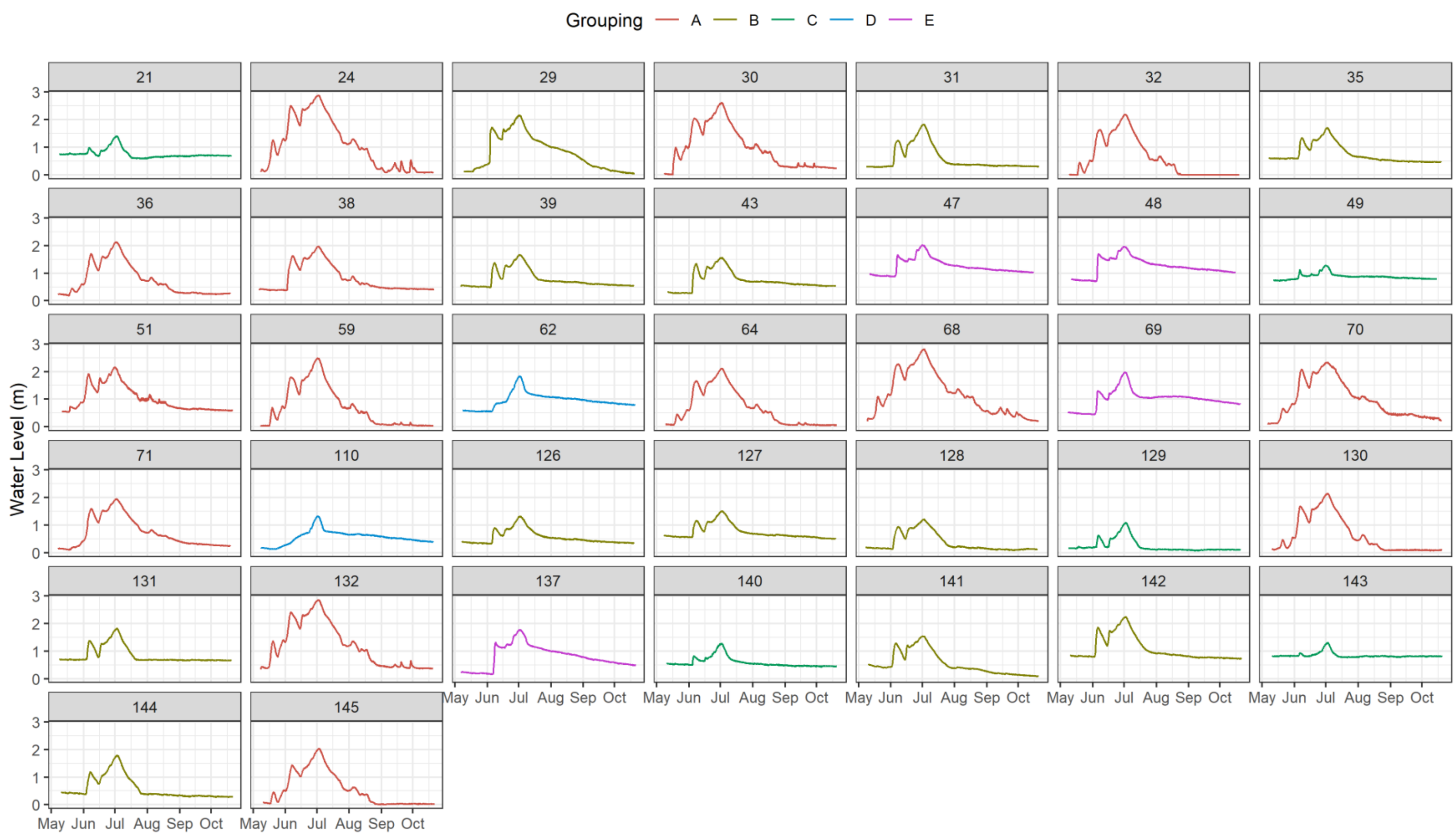


*Figure 5 Wetland water levels measured in 2021 at 37 sites within the upper Columbia floodplain. Wetlands were preliminarily arranged into five groups based on hydrograph response. Data from wetland 63 were not collected due to a malfunction.*

Maximum annual wetland water levels were higher in 2021 (Figure 5) compared to 2020 (Appendix Figure A1). Warm weather and rain-on-snow likely contributed to the first hydrograph peak from June 6 – 8, 2021 followed by the maximum annual peak around July 1 – 3, 2021. Based on the hydrograph response, wetlands were preliminarily grouped into five types (Figure 5), which was a similar grouping to 2020 (Appendix Figure A1). However, the wetland types were further characterized using geomorphic and hydrologic data collected in collaboration with University of Waterloo students and statistical analyses.

## 3.2 Principal Component Analysis

The PCA of wetland attributes found PC1 and PC2 carry 45% and 21% of the variance of the data (i.e., information), respectively (Figure 6). The variance of the data is explained in PC1 primarily between all hydrograph and geomorphic variables, while PC2 is explained by wetland storage and conductivity variables (Table 1). Over four principal components, the results explain 89% of variance in the data. The wetlands were plotted along the principal component axes to explore and visualize wetland grouping (Figure 6).

*Table 1 Principal component analysis of hydrograph, geomorphic and conductivity (CondMay) variables. Storage is the total change in wetland storage; Flashiness is how quickly the water level rises and falls during the season; Recession1 is the recession rate of the early June peak; Recession2 is the recession rate of the maximum annual peak flow; and ,TFGapW is the total gap width that allow water to inflow or outflow.*

| Principal Component | 1 | 2 | 3 | 4 | 5 | 6 | 7 |
|---|---|---|---|---|---|---|---|
| Storage | 0.7 | 51.3 | 0.4 | 23.1 | 18.0 | 1.4 | 5.2 |
| Flashiness | 23.7 | 1.1 | 7.3 | 15.5 | 5.0 | 0.6 | 46.9 |
| Recession1 | 16.4 | 4.3 | 19.5 | 10.9 | 33.2 | 14.8 | 0.9 |
| Recession2 | 24.8 | 0.3 | 7.9 | 1.0 | 18.4 | 6.2 | 41.3 |
| DamNo10 | 13.7 | 0.2 | 44.5 | 0.0 | 2.5 | 37.4 | 1.7 |
| TFGapW | 18.8 | 1.0 | 20.3 | 0.4 | 21.4 | 37.6 | 0.5 |
| CondMay | 2.0 | 41.8 | 0.1 | 49.1 | 1.6 | 1.9 | 3.5 |
| Eigenvalues | 3.14 | 1.48 | 0.99 | 0.61 | 0.35 | 0.31 | 0.12 |
| Proportion (%) | 45 | 66 | 80 | 89 | 94 | 98 | 100 |

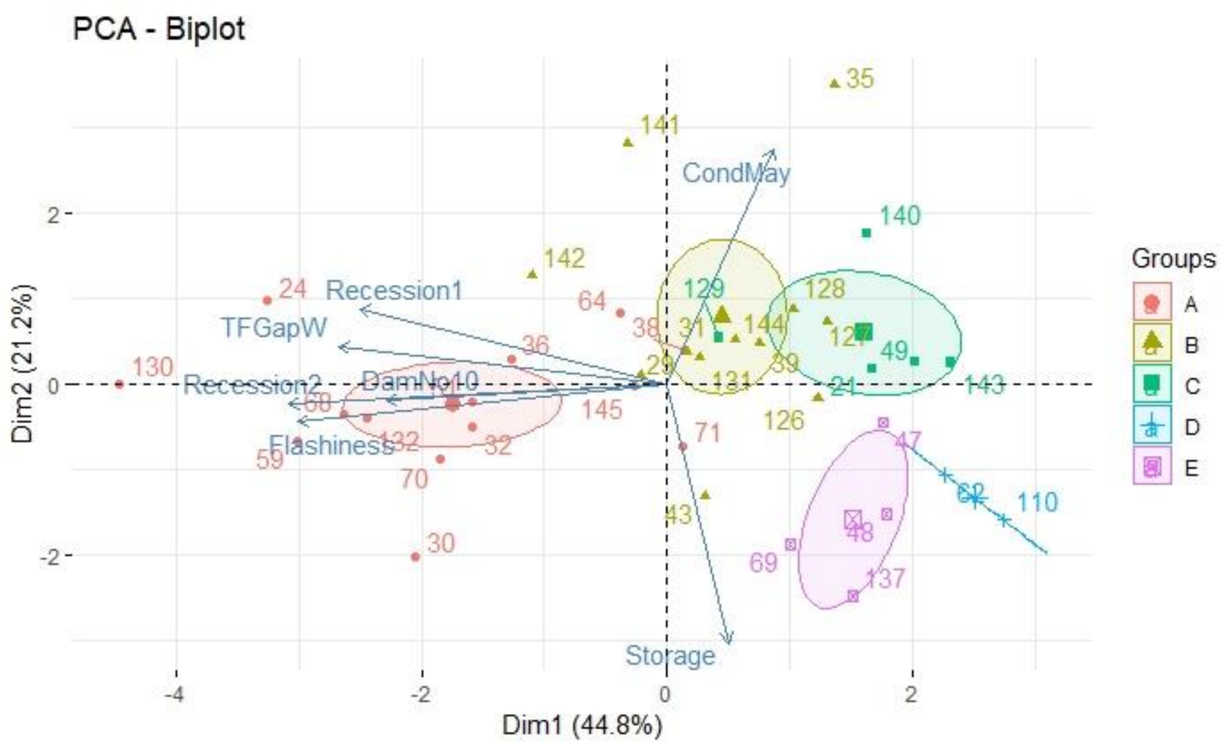


*Figure 6 Wetlands plotted along the PC 1 (i.e., Dim1) and PC2 (i.e., Dim2) axes. The larger symbols indicate the mean of the group.*

## 3.3 Wetland Types

A framework of first-order controls and wetland variables were used to group the wetlands into three types based on the wetland's connectivity to the channel network: continuous connectivity, discontinuous connectivity and no connectivity (Table 2 and Figure 5).

### 3.3.1 Continuous Connectivity

Wetlands with a group A hydrograph response have a relatively high degree of hydrologic connectivity with the channel network. Geomorphic data indicates all wetlands are connected to the main river channel via a gap in the levee. Water levels in these wetlands have a similar hydrograph response to water levels measured in the Columbia River at Spillimacheen Bridge (Figure 2). Therefore, these wetlands experience water level fluctuations as river flow rises and falls (i.e., flashier).

### 3.3.2 Discontinuous Connectivity

Wetlands in this type appear to have an inlet/outlet with inflow and outflow dependent on the elevation of a beaver dam (overdam flooding) or the bank elevation of the gap in the levee (overbank flooding) or the bank elevation of the adjacent wetland (overbank flooding), where the adjacent wetland is connected via gaps to the channel network. Geomorphic data indicate most wetlands have gaps that allow inflow of river, creek or adjacent wetland surface water, but the rate and magnitude of inflow is dependent on exceeding the elevation threshold.

The wetland water levels in group B typically did not show a response until the early June peak and had a faster maximum annual peak recession rate, while wetland water levels in group C had a more subdued response during the early June peak and maximum annual peak events. The differences in response between group B and C are likely due to the elevation threshold and the water level needed to exceed the threshold for flooding. These wetlands also had a faster recession rate compared to hydrographs of groups D and E, which may be due to an apparent outlet that allows water to more easily drain. This wetland type is less connected to the channel network via surface pathways and the water level changes would be a result of overbank (overdam) flooding, groundwater inflow, drainage and loss to evapotranspiration.

### 3.3.3 No Connectivity

Wetlands in this type are not directly connected to the channel network via gaps in the levee. Geomorphic data indicates there were no gaps that moved water into these wetlands. Rather, wetlands likely respond to unchannelized surface inflow as a result of over-levee flooding as the river stage rises. The wetland water levels in group E did show a response to the early June peak event and had a slower maximum annual peak recession rate that resulted in a higher water level at the end of the season compared to the spring. In contrast, group D had no distinct early June peak response likely due to the influence of dams, but had a slow maximum annual peak recession rate similar to group E. The slow drainage and higher storage in this wetland type is likely a result of no apparent outlet. These wetlands would experience high rates of evapotranspiration in the summer period.

*Table 2 Description of topology (i.e., refers to degree of hydrologic connectivity with the main channel network and degree of connectivity over space and time), typology (i.e., refers to the hydrograph response, which infers the predominant hydrologic fluxes and relative residence time of water held in wetland), and topography (i.e., refers to geomorphic setting of the wetland).*

| Topology | Typology | Topography | Wetland |
|---|---|---|---|
| Continuous connectivity | Response fluctuates with rise & fall of river stage | River gap | Group A: 24, 30, 32, 36, 38, 51, 59, 64, 68, 70, 71, 130, 132, 145, |
| Discontinuous connectivity | Responds post-overbank or overdam flooding, easily drains overflow | River gap, creek gap or between wetland gap; gap and/or dam elevation | Group B: 29, 31, 35, 39, 43, 126, 127, 128, 131, 141, 142, 144<br><br>Group C: 21, 49, 129, 140, 143 |
| No connectivity | Responds post-overlevee (overdam) flooding, slow drainage | No gap; levee (or dam) elevation | Group D: 62, 110<br><br>Group E: 47, 48, 69, 137 |

## 3.4 Wetland Water Balances

Total rainfall was 152 mm during the May 15 – Sep 30, 2021 study period, while total open-water evaporation was estimated to be 920 mm. Open-water evaporation at the Columbia wetlands was compared to E estimates at Upper Klamath Lake, Oregon, which is located in a semi-arid region of the

Cascade Range and receives about 100 mm less annual precipitation (mean annual precipitation 365 mm; Stannard et al., 2013). The three-month total at Upper Klamath Lake (636 mm) was close for the similar time period at the Columbia wetlands (735 mm), where the maximum E rate was 7 mm $d^{-1}$ at Upper Klamath Lake and 12.5 mm $d^{-1}$ at the Columbia wetlands.

The total growing season water balance by type indicated continuously connected wetlands (group A) had the greatest Net value compared to the other groups (Figure 7 Conceptual wetland water balances for wetlands continuously connected (group A), discontinuously connected (group B and C) and not connected (group D and E) to the channel network. Values represent the total growing season and are presented in $m^3$ with mm in brackets. Figure 7). Continuously connected wetlands also had the lowest P:E ratio (1:3.1) compared to wetlands that are not connected (1:4.1) and discontinuously connected (1:4.0). Total growing season water balances calculated for 2020 by wetland type showed a similar trend (Appendix Figure A3, Table A2).

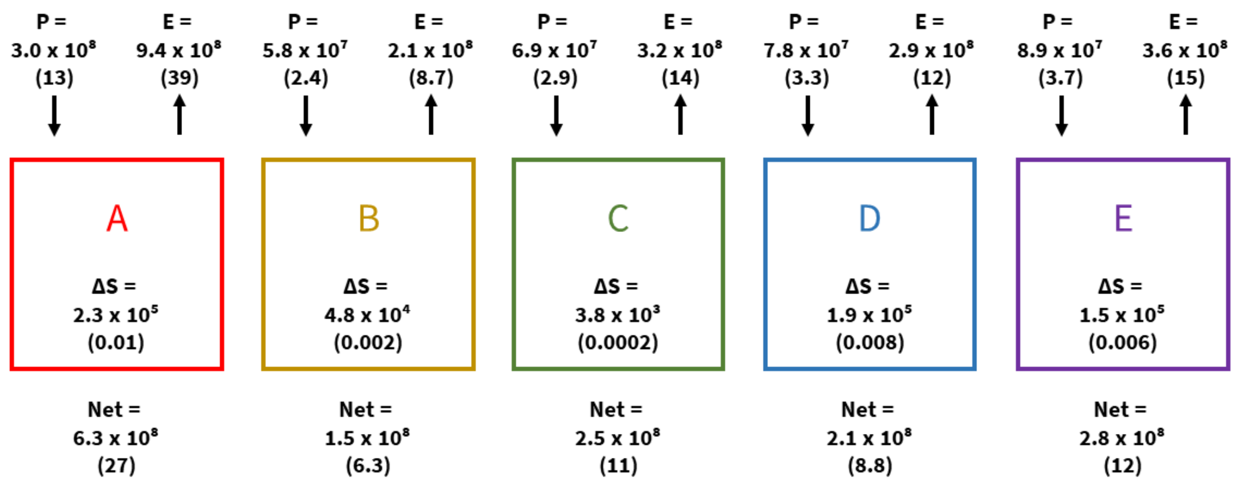


*Figure 7 Conceptual wetland water balances for wetlands continuously connected (group A), discontinuously connected (group B and C) and not connected (group D and E) to the channel network. Values represent the total growing season and are presented in $m^3$ with mm in brackets.*

## 3.5 Wetland Vulnerability to Climate Change

For the northern hemisphere, warmer air temperatures associated with climate change are expected to alter precipitation and evapotranspiration patterns (Feulner et al., 2013). For areas within the Upper Columbia Basin that are characterized by high elevations, cold air temperatures, high precipitation and glaciers will be particularly vulnerable since these future climate conditions will further accelerate glacier retreat (MacDonald Hydrology Consultants, 2020). Changes in climate will affect streamflow in both the high-elevation and low-elevation areas of the watershed, which will affect the hydrologic inputs to the wetlands.

Climate change scenarios project average annual air temperature increases for the study area (1.4 – 1.7°C by 2050, 2.4 – 3.6°C by 2080; Figure 4). Precipitation is projected to slightly increase (27 – 35 mm by 2050, 53 – 70 mm by 2080; Figure 4), but the change in the timing (and amount) and phase of precipitation will have the larger impact on wetland hydrology. There is an expected reduction in the fraction of annual precipitation that falls as snow (4 – 6% by 2050, 9 – 14% by 2080; Figure 4). Reduction of snowfall at high-elevation would be critical for late-season streamflow. Already, Columbia River flows at Nicholson have declined 13% in recent decades (Brahney et al, 2017), with much of the decline in August (Moore et al., 2020).

Wetlands in the lowlands of mountain landscapes receive their water primarily from groundwater discharge and the stream network (Winter, 2000). Given that the wetlands are in the Upper Columbia River floodplain, near the headwaters of both streams and groundwater flow systems, the upgradient watersheds of either water source are relatively small, which makes the region more vulnerable to changes in climate. All wetlands in the upper Columbia River floodplain will likely be vulnerable to climate change, but at different time scales given that both streams and groundwater flow systems are snowmelt (glacier)-dominated.

Projected climate change would shift the watershed towards more rainfall-dominated runoff and result in earlier snowmelt and spring peak flows, which may change the timing and duration of overbank/overdam/overlevee flooding and the period of inundation. Some wetlands not continuously connected to the river channel do not receive as much inflow during the maximum annual peak flows (flood <0.5 - 1 m; Figure 5; Figure A1) compared to those that are continuously connected (flood 2-3 m during maximum annual peak flow). Therefore, with projected climate change, the more isolated wetlands would flood less and there would be concerns that a wetland under an extended growing season with greater evapotranspiration rates would not retain as much standing water over the winter and be particularly vulnerable to climate change.

At the wetland-scale, wetlands continuously connected via surface pathways (group A) would be less vulnerable to climate change. Although the fraction of snowfall will likely decrease, an increase in precipitation (as rain) will likely be able to maintain this wetland type despite a likely increase in E from warmer air temperatures. Wetlands that have discontinuous connectivity with the channel network (group B, C) would be more vulnerable to warmer air temperatures (increased E) and a shift in precipitation phase from snowfall to rainfall, which could shift the timing and magnitude of the peak flows. Water levels that do not exceed the elevation of the gap bank or dam would increase the vulnerability of the discontinuously connected wetlands by reducing the volume of water within the wetland. Groundwater inflow would then be needed to maintain the wetland water level with an increase in E. However, groundwater inflow rates would depend on the wetland's hydrogeologic setting and groundwater flow system. This would be a similar situation for wetlands not connected to the channel network (group E), which depend on the river stage to exceed the levee elevation to flood the wetland. Therefore, how well (e.g., duration, timing) a wetland is connected to the channel network and how connectivity varies with changes in streamflow will determine the vulnerability to climate change. Wetlands that have discontinuous connectivity or no connectivity would be the most vulnerable and most important to mitigate to maintain habitat quality and bioecological functioning of the wetland.

# 4 Conclusion

This report has presented further analyses to group monitored wetlands into types and provided a conceptual understanding of predominant water sources and fluxes within each wetland type. This information was used to evaluate wetlands that are most (or least) vulnerable to climate change. Next steps in the project are to model the wetland response to climate change and select wetlands to mitigate climate change impacts using artificial beaver dams or an alternate mitigation approach**.**

Recommendations for further work include:

- Refine the volume-elevation and surface area-elevation curves by conducting further bathymetric surveys for a selected sample of wetlands in 2022;
- Continue monitoring wetland water levels in 2022;
- Consider collection of a water isotope sample from each wetland to help evaluate contribution of water budget components as current conceptual understanding lumps surface and groundwater inflow/outflow together because field measurement of these fluxes is not easy. Water samples could be used to calculate an Evaporation/Inflow ratio as well as contribution from groundwater based on a mixing model developed from 2019/2020 isotope data collection; and,
- Evaluate changes in source water terms as a function of climate and land use change using a hydrologic model.

# 5 References

Brahney, J., Weber, F., Foord, V., Janmaat, J., & Curtis, P. J. (2017). Evidence for a climate-driven hydrologic regime shift in the Canadian Columbia Basin. Canadian Water Resources Journal/Revue canadienne des ressources hydriques, 42(2), 179-192.

Buttle, J. (2006). Mapping first-order controls on streamflow from drainage basins: the T3 template. Hydrological Processes, 20(15), 3415-3422.

Dingman, S., 2002. Physical Hydrology. Waveland Press Inc.

Environment and Climate Change Canada (ECCC). (2021). CMIP5 statistically downscaled climate scenarios. *https://climate-scenarios.canada.ca/?page=statistical-downscaling*

Feulner, G., Rahmstorf, S., Levermann, A., & Volkwardt, S. (2013). On the origin of the surface air temperature difference between the hemispheres in Earth's present-day climate. Journal of Climate, 26(18), 7136-7150.

Hayashi, M., & Van der Kamp, G. (2000). Simple equations to represent the volume–area–depth relations of shallow wetlands in small topographic depressions. Journal of hydrology, 237(1-2), 74-85.

Hopkinson, C., Fuoco, B., Grant, T., Bayley, S. E., Brisco, B., & MacDonald, R. (2020). Wetland Hydroperiod Change Along the Upper Columbia River Floodplain, Canada, 1984 to 2019. Remote Sensing, 12(24), 4084.

MacDonald Hydrology Consultants Ltd. 2021. Interim Report – Upper Columbia Wetland Vulnerability Assessment. Prepared for: Columbia Wetland Stewardship Partners. 23 pp.

MacDonald Hydrology Consultants Ltd. 2020. Hydrological Assessment of the Upper Columbia River Watershed. 64 pp. Submitted February 2020 to Columbia Wetlands Stewardship Partners.

McMahon, T. A., Peel, M. C., Lowe, L., Srikanthan, R., & McVicar, T. R. (2013). Estimating actual, potential, reference crop and pan evaporation using standard meteorological data: a pragmatic synthesis. Hydrology and Earth System Sciences, 17(4), 1331-1363.

Moore, R. D., Pelto, B., Menounos, B., & Hutchinson, D. (2020). Detecting the effects of sustained glacier wastage on streamflow in variably glacierized catchments. Frontiers in Earth Science, 8, 136.

Penman, H. L. (1948). Natural evaporation from open water, bare soil and grass. Proceedings of the Royal Society of London. Series A. Mathematical and Physical Sciences, 193(1032), 120-145.

Remer, C.R., Rooney, R., Bolding, M., Leven, C., & Bayley, S. (in prep). Hydrological processes of wetlands in the Columbia River floodplain.

Stannard, D.I., Gannett, M.W., Polette, D.J., Cameron, J.M., Waibel, M.S., & Spears, J.M. (2013). Evapotranspiration from marsh and open-water sites at Upper Klamath Lake, Oregon, 2008–2010: U.S. Geological Survey Scientific Investigations Report 2013–5014, 66 p.

Winter, T. C. (2000). The vulnerability of wetlands to climate change: a hydrologic landscape perspective 1. JAWRA Journal of the American Water Resources Association, 36(2), 305-311.

Zhang, X., Flato, G., Kirchmeier-Young, M., Vincent, L., Wan, H., Wang, X., Rong, R., Fyfe, J., Li, G., Kharin, V.V. (2019): Changes in Temperature and Precipitation Across Canada; Chapter 4 in Bush, E. and

Lemmen, D.S. (Eds.) Canada's Changing Climate Report. Government of Canada, Ottawa, Ontario, pp 112-193.

# 6 Appendix

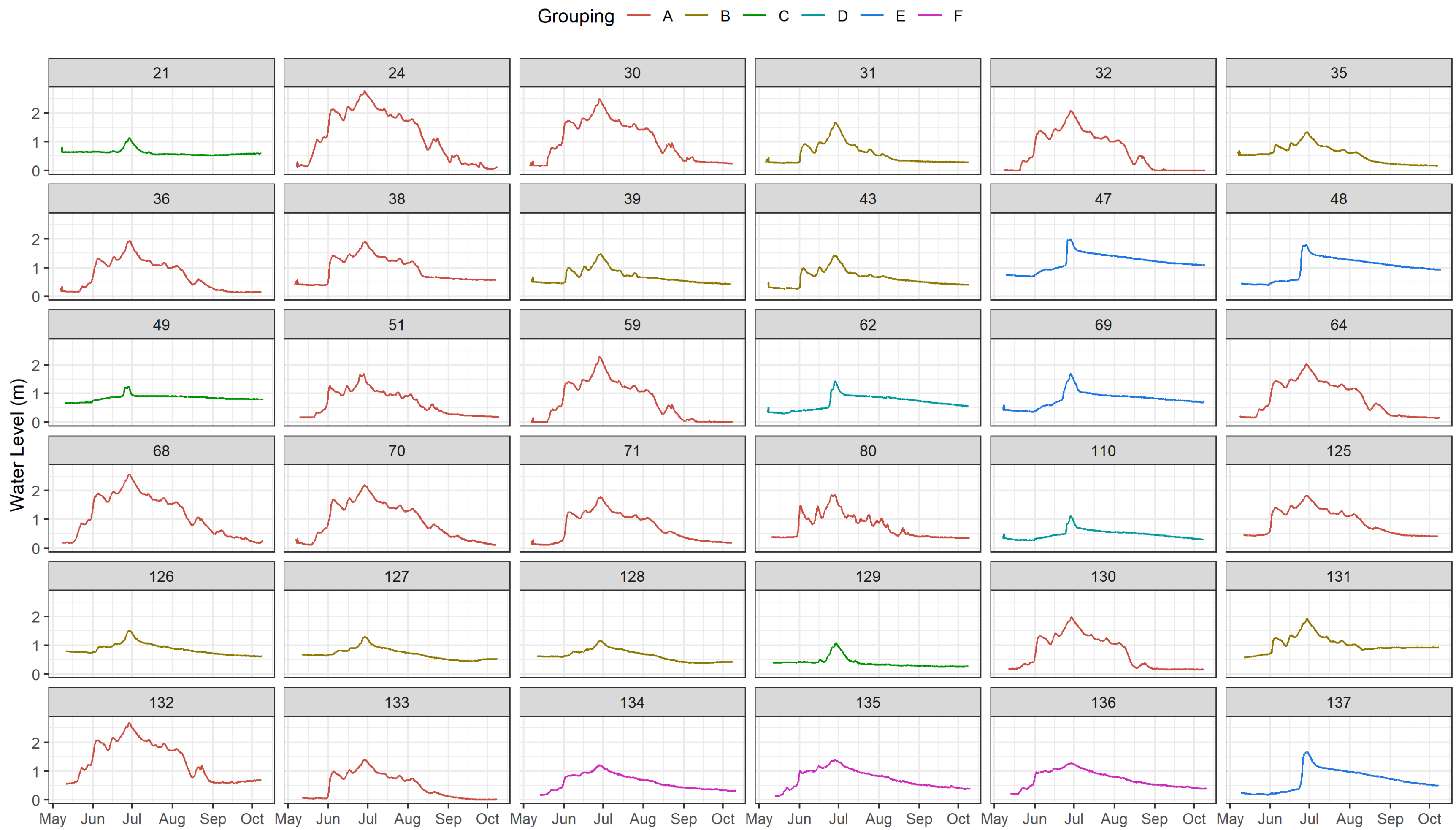


*Figure A1 Wetland water levels measured in 2020 at 36 sites within the upper Columbia floodplain. Wetlands were preliminarily arranged into six groups based on hydrograph response. Group F (wetlands 134, 135, and 136) were dropped in 2021.*

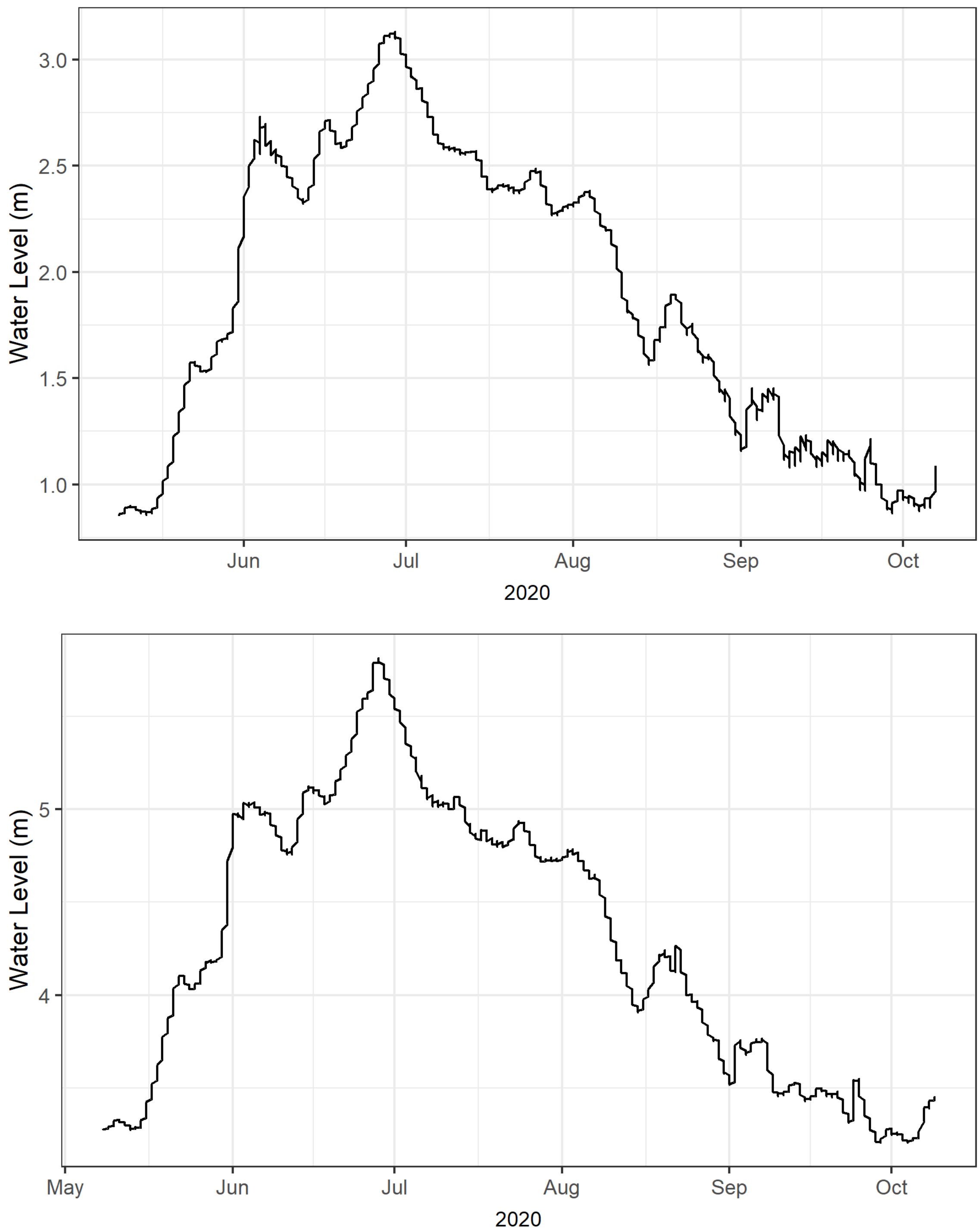


*Figure A2 Water levels in the Columbia River at Brisco (top) and at the Spillimacheen Bridge (bottom) in 2020.*

*Table A1 Total monthly 2021 water balance for wetland types: continuous connectivity (group A), discontinuous connectivity (group B and C) and no connectivity (group D and E). Volumetric values were divided by the total wetland area in 2021 (23,830,766 $m^2$).*

| | **A** | | **B** | | **C** | | **D** | | **E** | |
|---|---|---|---|---|---|---|---|---|---|---|
| | **$m^3$** | **mm** | **$m^3$** | **mm** | **$m^3$** | **mm** | **$m^3$** | **mm** | **$m^3$** | **mm** |
| | | | | | **June** | | | | | |
| P | 7.3E+07 | 3.1 | 1.4E+07 | 0.6 | 1.7E+07 | 0.7 | 1.9E+07 | 0.8 | 2.2E+07 | 0.9 |
| E | 3.7E+08 | 15.6 | 7.0E+07 | 2.9 | 9.2E+07 | 3.9 | 7.9E+07 | 3.3 | 1.1E+08 | 4.6 |
| ΔS | 3.4E+06 | 0.1 | 6.1E+05 | 0.0 | 3.2E+05 | 0.0 | 8.5E+05 | 0.0 | 9.0E+05 | 0.0 |
| Net | 3.0E+08 | 12.7 | 5.6E+07 | 2.4 | 7.6E+07 | 3.2 | 6.0E+07 | 2.5 | 8.8E+07 | 3.7 |
| | | | | | **July** | | | | | |
| P | 1.6E+07 | 0.7 | 3.1E+06 | 0.1 | 3.7E+06 | 0.2 | 4.2E+06 | 0.2 | 4.8E+06 | 0.2 |
| E | 3.8E+08 | 15.9 | 7.4E+07 | 3.1 | 1.0E+08 | 4.3 | 1.1E+08 | 4.5 | 1.3E+08 | 5.5 |
| ΔS | -3.2E+06 | -0.1 | -5.0E+05 | 0.0 | -3.3E+05 | 0.0 | -4.9E+05 | 0.0 | -5.4E+05 | 0.0 |
| Net | 3.6E+08 | 15.0 | 7.0E+07 | 2.9 | 9.9E+07 | 4.2 | 1.0E+08 | 4.3 | 1.3E+08 | 5.3 |
| | | | | | **August** | | | | | |
| P | 1.1E+08 | 4.4 | 2.0E+07 | 0.8 | 2.4E+07 | 1.0 | 2.7E+07 | 1.1 | 3.1E+07 | 1.3 |
| E | 9.9E+07 | 4.1 | 3.0E+07 | 1.2 | 5.3E+07 | 2.2 | 5.0E+07 | 2.1 | 5.9E+07 | 2.5 |
| ΔS | -1.1E+06 | 0.0 | -2.7E+04 | 0.0 | 9.3E+03 | 0.0 | -6.4E+04 | 0.0 | -9.1E+04 | 0.0 |
| Net | -8.2E+06 | -0.3 | 9.4E+06 | 0.4 | 2.9E+07 | 1.2 | 2.3E+07 | 1.0 | 2.8E+07 | 1.2 |
| | | | | | **September** | | | | | |
| P | 6.4E+07 | 2.7 | 1.2E+07 | 0.5 | 1.4E+07 | 0.6 | 1.7E+07 | 0.7 | 1.9E+07 | 0.8 |
| E | 3.7E+07 | 1.5 | 1.9E+07 | 0.8 | 3.7E+07 | 1.6 | 3.2E+07 | 1.3 | 3.8E+07 | 1.6 |
| ΔS | -1.2E+05 | 0.0 | -3.4E+04 | 0.0 | -1.0E+04 | 0.0 | -8.8E+04 | 0.0 | -7.6E+04 | 0.0 |
| Net | -2.8E+07 | -1.2 | 7.2E+06 | 0.3 | 2.3E+07 | 1.0 | 1.5E+07 | 0.6 | 1.9E+07 | 0.8 |

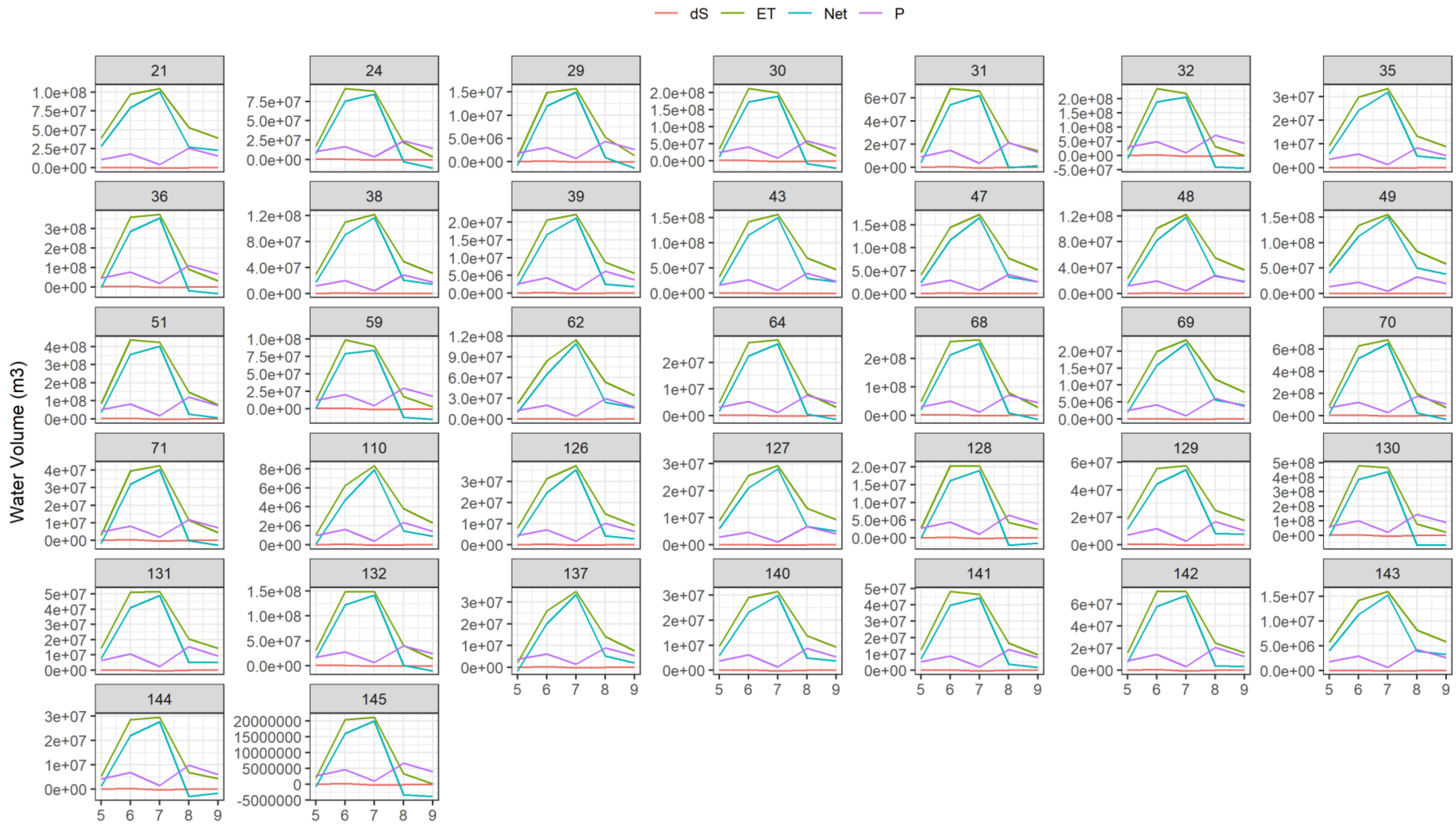


*Figure A3 Time series of volumetric water balance terms from May 15 – Sep 30, 2021 for all monitored wetlands.*

*Table A2 Total growing season water balance (May 15 – Sep 30, 2020) for wetland types: continuous connectivity (group A), discontinuous connectivity (group B and C) and no connectivity (group D and E). Volumetric values were divided by the total wetland area in 2020 (22,559,970 $m^2$).*

| | A | | B | | C | | D | | E | |
|---|---|---|---|---|---|---|---|---|---|---|
| | **$m^3$** | **mm** | **$m^3$** | **mm** | **$m^3$** | **mm** | **$m^3$** | **mm** | **$m^3$** | **mm** |
| P | 2.3E+08 | 10.4 | 4.9E+07 | 2.2 | 5.9E+07 | 2.6 | 6.0E+07 | 2.7 | 6.8E+07 | 3.0 |
| E | 7.6E+08 | 33.7 | 2.1E+08 | 9.2 | 3.3E+08 | 14.6 | 2.0E+08 | 8.9 | 3.0E+08 | 13.3 |
| ΔS | 3.8E+04 | 0.0 | 4.6E+04 | 0.0 | 1.5E+04 | 0.0 | 1.8E+05 | 0.0 | 3.2E+05 | 0.0 |
| Net | 5.3E+08 | 23.3 | 1.6E+08 | 7.1 | 2.7E+08 | 12.0 | 1.4E+08 | 6.3 | 2.3E+08 | 10.3 |

*Table A3 Total monthly 2020 water balance for wetland types: continuous connectivity (group A), discontinuous connectivity (group B and C) and no connectivity (group D and E). Volumetric values were divided by the total wetland area in 2020 (22,559,970 $m^2$).*

| | A | | B | | C | | D | | E | |
|---|---|---|---|---|---|---|---|---|---|---|
| | **$m^3$** | **mm** | **$m^3$** | **mm** | **$m^3$** | **mm** | **$m^3$** | **mm** | **$m^3$** | **mm** |
| | | | | | **June** | | | | | |
| P | 7.9E+07 | 3.5 | 1.7E+07 | 0.7 | 2.0E+07 | 0.9 | 2.0E+07 | 0.9 | 2.3E+07 | 1.0 |
| E | 2.7E+08 | 12.0 | 6.0E+07 | 2.6 | 7.9E+07 | 3.5 | 4.0E+07 | 1.8 | 6.0E+07 | 2.6 |
| ΔS | 2.7E+06 | 0.1 | 5.7E+05 | 0.0 | 2.1E+05 | 0.0 | 5.8E+05 | 0.0 | 8.5E+05 | 0.0 |
| Net | 1.9E+08 | 8.6 | 4.4E+07 | 1.9 | 5.9E+07 | 2.6 | 2.0E+07 | 0.9 | 3.8E+07 | 1.7 |
| | | | | | **July** | | | | | |
| P | 3.9E+07 | 1.7 | 8.1E+06 | 0.4 | 9.7E+06 | 0.4 | 9.9E+06 | 0.4 | 1.1E+07 | 0.5 |
| E | 2.8E+08 | 12.3 | 6.1E+07 | 2.7 | 8.8E+07 | 3.9 | 6.4E+07 | 2.8 | 9.7E+07 | 4.3 |
| ΔS | -1.8E+06 | -0.1 | -3.9E+05 | 0.0 | -1.8E+05 | 0.0 | -2.5E+05 | 0.0 | -3.0E+05 | 0.0 |
| Net | 2.4E+08 | 10.5 | 5.2E+07 | 2.3 | 7.8E+07 | 3.4 | 5.4E+07 | 2.4 | 8.6E+07 | 3.8 |
| | | | | | **August** | | | | | |
| P | 2.2E+07 | 1.0 | 4.6E+06 | 0.2 | 5.5E+06 | 0.2 | 5.7E+06 | 0.3 | 6.4E+06 | 0.3 |
| E | 1.5E+08 | 6.6 | 4.9E+07 | 2.2 | 8.4E+07 | 3.7 | 5.8E+07 | 2.6 | 8.5E+07 | 3.8 |
| ΔS | -1.9E+06 | -0.1 | -9.3E+04 | 0.0 | -2.8E+04 | 0.0 | -9.1E+04 | 0.0 | -1.4E+05 | 0.0 |
| Net | 1.2E+08 | 5.5 | 4.4E+07 | 1.9 | 7.9E+07 | 3.5 | 5.2E+07 | 2.3 | 7.9E+07 | 3.5 |
| | | | | | **September** | | | | | |
| P | 0.0E+00 | 0.0 | 0.0E+00 | 0.0 | 0.0E+00 | 0.0 | 0.0E+00 | 0.0 | 0.0E+00 | 0.0 |
| E | 2.8E+07 | 1.3 | 2.3E+07 | 1.0 | 4.4E+07 | 1.9 | 2.6E+07 | 1.2 | 4.0E+07 | 1.8 |
| ΔS | -3.7E+05 | 0.0 | -3.9E+04 | 0.0 | -4.8E+03 | 0.0 | -1.0E+05 | 0.0 | -1.0E+05 | 0.0 |
| Net | 2.8E+07 | 1.2 | 2.3E+07 | 1.0 | 4.4E+07 | 1.9 | 2.6E+07 | 1.2 | 4.0E+07 | 1.8 |

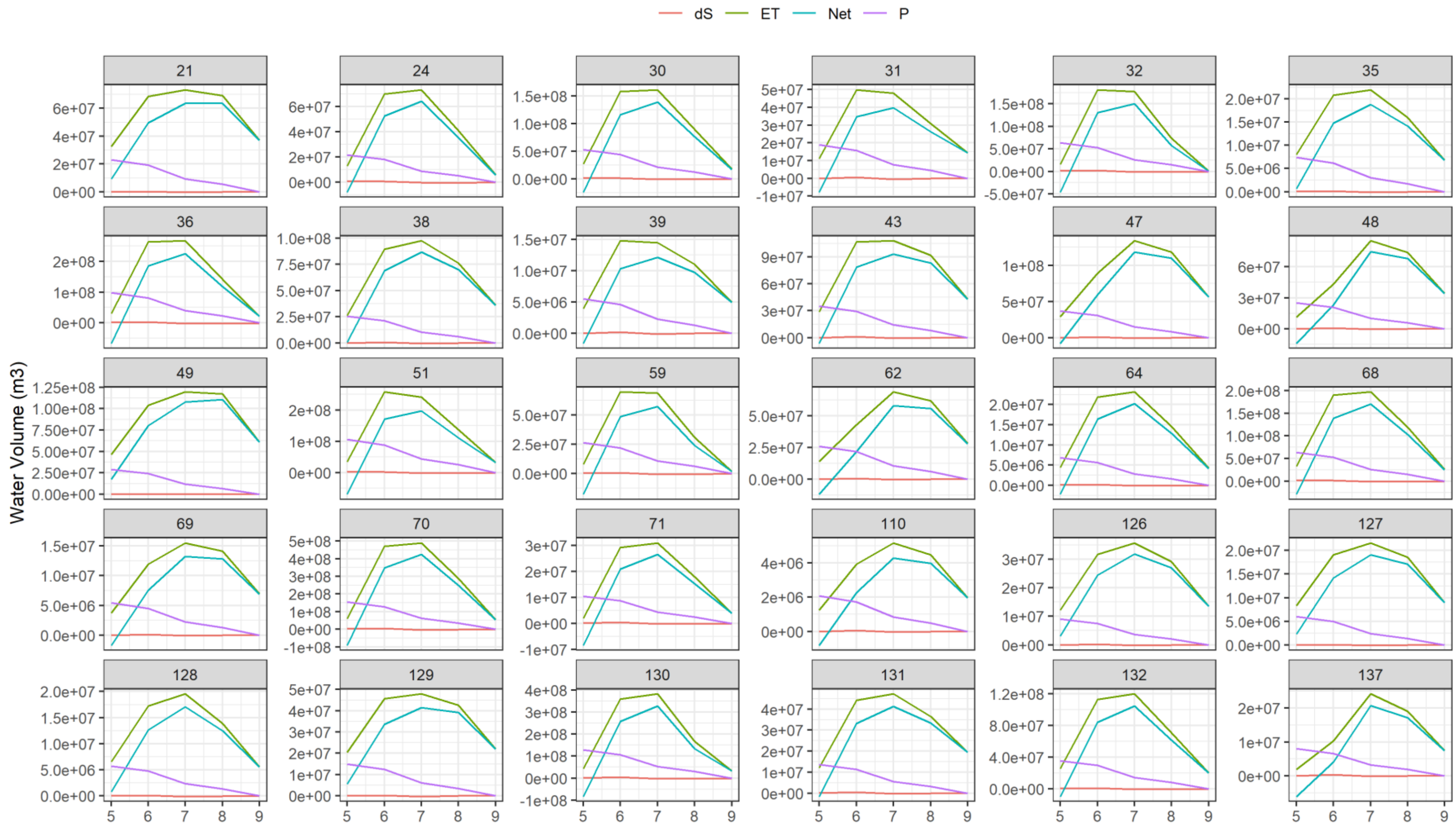


*Figure A4 Time series of volumetric water balance terms from May 15 – Sep 30, 2020 for all monitored wetlands.*